On the use of conservative formulation of energy equation in hybrid compressible lattice Boltzmann method

S. Guo, Y. Feng, Pierre Sagaut

On the use of conservative formulation of energy equation in hybrid compressible lattice Boltzmann method

S. Guo, Y. Feng*, P. Sagaut

Aix Marseille Univ, CNRS, Centrale Marseille, M2P2 UMR 7340, 13451 Marseille, France

ARTICLE INFO

Article history:
Received 20 May 2020
Revised 3 December 2020
Accepted 7 January 2021
Available online 27 January 2021

Keywords:
Hybrid LBM
Consistency
Mass conservation
Compressible flows

ABSTRACT

Effect of density variations on mass conservation properties is widely recognized in the lattice Boltzmann method (LBM), thus non-conservative form of scalar transport equation was commonly adopted within the framework of hybrid LBM. Focusing on the compressible hybrid LBM, mass conservation and its effect on energy conservation equation are studied in this paper. Starting from the analysis on mass conservation law recovered by LBM, the consistency between conservative and non-conservative formulations of energy conservation equation based on various thermodynamic variables and lattice Boltzmann equation is addressed. Driven by the theoretical analysis, a set of modified consistent energy equations in entropy and internal energy form is derived to reduce the error terms and improve the consistency. The theoretical analysis and modified energy equations are intensively evaluated by several numerical test cases, e.g., the isentropic vortex convection, three-dimensional compressible Taylor-Green vortex and shock-vortex interaction.

1. Introduction

The lattice Boltzmann method (LBM) has been proven to be a promising solver for the Navier-Stokes equations. Accounting for the numerical efficiency, hybrid LB methods were developed in multi-physics application as well as fully coupled compressible flows where mass and momentum conservation equation in the conservative forms are recovered and solved by the simple collision-streaming type LB method while the scalar transport or energy conservation equation is solved by using a finite volume method (FVM) or finite difference method (FDM). As summarized in Table 1, the non-conservative form of scalar transport equations or energy conservation equation are commonly used in the LB models for thermal flows, phase transition and multi-component transport applications. One explanation for that is that most of these models were derived for nearly-constant density flows, at least in each phase. On the other hand, the non-conservative form of additional conservation equations can decouple the numerical oscillation of density (or pressure, $p = \rho c_s^2$) and deviation of the mass conservation in the lattice Boltzmann solver.

The mass conservation is widely recognized as a key issue of the lattice Boltzmann method. The flaw of mass conservation can originate in several sources, for instance: 1) boundary condition treatment, 2) discretization of forcing terms and 3) higher-order contributions arising in Chapman-Enskog expansion. The error on mass conservation due to the treatment of boundary by using some physical assumptions or numerical approximation. The effect of implementation and discretization of forcing terms in lattice Boltzmann model was investigated by theoretical analysis and numerical experiments in several works [18–23]. The truncation error analysis based on the higher-order Chapman-Enskog expansion and Taylor series expansion was performed to present non-hydrodynamic terms in lattice Boltzmann method in several studies, where the different extra terms were derived thanks to individual interpretation of connection between the Boltzmann equation and the LB method [24].

Focusing on the compressible lattice Boltzmann models, the mass conservation flaw induced by the above mentioned factors and associated effects on the energy conservation law can significantly affect the numerical robustness and accuracy, accounting for the fully coupled thermodynamic closure. Recently, a set of hybrid LB model for the subsonic and supersonic compressible flows [4,5,25] has been developed on low-symmetry lattices with only 19+1 or 39+1 degrees of freedom per-node in three-dimensional flows. In this type of hybrid approach, the density and velocity are computed using the LB method with non-uniform forcing terms while the energy equation is solved using a finite volume/difference method.

Although the hybrid compressible lattice Boltzmann models have been used in a number of academic and industrial appli-

* Corresponding author.
E-mail address: yongliang.feng@univ-amu.fr (Y. Feng).

Table 1
Brief overview on formulation of additional scalar equations in hybrid LB methods. In column application, ⋆ denotes the LB model with a non-uniform forcing term. CF: conservative form, NCF: non-conservative form, I: intensity of radiation, P: phase of fluid, S: entropy, T: temperature, Y: mass component.

Refs.	form	scalars	application	compressi.
Lallemand & Luo [1]	NCF	T	convective flow	$Ma < 0.3$
Tölke & Latt [2]	NCF	T	thermal flow	$Ma < 0.3$
Gupta et al. [3]	NCF⋆	Y	multicomponent	$Ma < 0.3$
Nie et al. [4]	NCF⋆	S	aerodynamic flow	$Ma < 1.8$
Feng et al. [5]	NCF⋆	S	aerodynamic flow	$Ma < 1.0$
Mezrhab et al. [6]	NCF	T	natural convection	$Ma < 0.3$
Sun et al. [7]	NCF	T & I	thermal flow	$Ma < 0.3$
Marenduzzo et al. [8]	NCF	P	liquid crystal	$Ma < 0.3$
Li et al. [9]	NCF⋆	T	multiphase flow	$Ma < 0.3$
Nee [10]	NCF⋆	T	natural convection	$Ma < 0.3$
Bettaibi et al. [11]	NCF	T &Y	convective flow	$Ma < 0.3$
Qin et al. [12]	NCF⋆	T	liquid evaporation	$Ma < 0.3$
Wang et al. [13]	NCF⋆	T & P	natural convection	$Ma < 0.3$
Hosseini et al. [14]	NCF⋆	T & Y	combustion	$Ma < 0.3$
Yu et al. [15]	NCF	Y	mass transfer	$Ma < 0.3$
Filippova et al. [16]	NCF⋆	T & Y	combustion	$Ma < 0.3$
Chakraborty et al. [17]	CF⋆	T	phase transition	$Ma < 0.3$

cations [26,27], selecting a formulation for the energy conservation law and associated numerical properties is still an open issue. In the present study, a high-order Chapman-Enskog expansion is performed to analyze the mass conservation flaw in the compressible LB method, the consistency between conservative and non-conservative energy conservation equations based on various thermodynamics variables and lattice Boltzmann equation is addressed. Theoretical analysis is supplemented by numerical experiments in a second step.

This paper is organized as follows. The key elements of hybrid compressible LBM are reminded in Section 2. A revised Chapman-Enskog expansion is also presented by considering the truncation error of forcing terms. Section 3 addresses the consistency between conservative and non-conservative energy conservation equations in the form of various thermodynamics variables and lattice Boltzmann equation. A set of consistent energy equations in entropy and internal energy form is also proposed in Section 3 to reduce the error terms and improve the consistency. The theoretical analysis and revised energy equations are intensively evaluated in Section 4 by several numerical test cases, e.g., the isentropic vortex convection, three-dimensional compressible Taylor-Green vortex and shock-vortex interaction. Finally, Section 5 draws conclusion and perspectives.

2. Hybrid lattice Boltzmann method

2.1. Lattice Boltzmann kernel for mass and momentum conservation

The lattice Boltzmann method describes the behavior of fluid flows in terms of density distribution functions $f_i(\boldsymbol{x}, t)$ on discrete time t, space $\boldsymbol{x}$ and velocities $\boldsymbol{c}_i$. The distribution functions evolve according to the lattice Boltzmann equation. The most common form of the LB equation, which uses the Bhatnagar-Gross-Krook (BGK) model [28,29]:

$$f_i(\boldsymbol{x}+\boldsymbol{\delta_x}, t+\delta_t) = f_i(\boldsymbol{x}, t) - \frac{1}{\tau}(f_i(\boldsymbol{x}, t) - f_\alpha^{\mathrm{eq}}(\boldsymbol{x}, t)) + \psi_i \tag{1}$$

where ψ_i is a generic force term. and the τ is the dimensionless relaxation time which is linked with fluid dynamic viscosity by $\mu = p(\tau - 0.5)\delta_t$ with p being pressure.

In the present study of hybrid compressible LB model, a third-order expansion of the equilibrium distribution function f_i^{eq} on the nearest-neighbour type lattices (D2Q9, D3Q19 and D3Q27) is used, which is expressed as

$$f_i^{eq} = w_i\left[\rho + \frac{\boldsymbol{c}_i}{c_s^2}\rho\boldsymbol{u} + \frac{\mathcal{H}_i^{(2)}}{2c_s^4}\mathcal{A}^{(2)} + \frac{\mathcal{H}_i^{(3)}}{6c_s^6}\mathcal{A}^{(3)}\right]. \tag{2}$$

where w_i is the i_{th} weight coefficient associated to discrete velocity $\boldsymbol{c}_i$, c_s is lattice sound speed and the discrete Hermite polynomials are given as $\mathcal{H}_i^{(2)} = \boldsymbol{c}_i\boldsymbol{c}_i - c_s^2\boldsymbol{\delta}$, $\mathcal{H}_i^{(3)} = \boldsymbol{c}_i\boldsymbol{c}_i\boldsymbol{c}_i - c_s^2[\boldsymbol{c}_i\boldsymbol{\delta}]$ and $\mathcal{A}^{(2)}$, $\mathcal{A}^{(3)}$ are respectively the second and third-order term coefficients of Hermite polynomials [5]. It is worth noting that the equilibrium distribution function f^{eq} can be accordingly improved on D3Q19 lattice [25].

The macroscopic quantities such as density ρ and momentum $\rho\boldsymbol{u}$ at the time step $t + \delta_t$ are updated by distribution functions in their velocity moments,

$$\rho = \sum_i f_i \tag{3a}$$

$$\rho\boldsymbol{u} = \sum_i \boldsymbol{c}_i f_i + \frac{\delta_t}{2}\sum_i \boldsymbol{c}_i\psi_i \tag{3b}$$

The correction term $\psi_i = -\frac{w_i}{2c_s^4}\mathcal{H}_i^{(2)}\nabla\boldsymbol{\Psi}^{(3)}$ is introduced in the forcing term to compensate symmetry-breaking errors $\boldsymbol{\Psi}^{(3)}$, which is due to the topology of the nearest-neighbour lattice [5,25]. On D3Q27 lattice, $\boldsymbol{\Psi}^{(3)} = \boldsymbol{0}$ except for $\boldsymbol{\Psi}^{(3)}_{\alpha\alpha\alpha} = \rho u_\alpha(\theta - 1 + u_\alpha^2)$, ($\alpha$ represents component of Cartesian coordinate without summation over repeated index). The simplified correction terms according to the revised equilibrium distribution function on D3Q19 lattice can refer to [25].

2.2. Revised Chapman-Enskog expansion

In order to analyze macroscopic equations taking into account higher-order truncation errors of correction forcing terms, the Chapman-Enskog analysis is revised in this section.

The semi-discrete Boltzmann equation used in Chapman-Enskog expansion can be derived from fully discrete lattice Boltzmann equation by three approaches: Taylor expansion approach, characteristics integration approach of He et al. [30] and Strang splitting operator of Dellar [24]. As a more common approach, the Taylor expansion is used to recast discrete Boltzmann equation from the Boltzmann equation in this study. Performing the third-order Taylor series expansion of lattice Boltzmann equation, the following discrete Boltzmann equation with truncation error terms can be obtained

$$\mathrm{D}_i f_i + \frac{\delta_t}{2}\mathrm{D}_i^2 f_i + \frac{\delta_t^2}{6}\mathrm{D}_i^3 f_i = -\frac{1}{\tau\delta_t}(f_i - f_i^{eq}) + \psi_i + \mathcal{O}(\delta_t^3) \tag{4}$$

where $D_i = \partial_t + \boldsymbol{c}_i\nabla$. The density distribution function f_i is expanded around the f_i^{eq} distributions as follows:

$$f_i = f_i^{(0)} + \epsilon f_i^{(1)} + \epsilon^2 f_i^{(2)} + \epsilon^3 f_i^{(3)} + \cdots \tag{5}$$

$$\frac{\partial}{\partial t} = \epsilon\frac{\partial}{\partial t_1} + \epsilon^2\frac{\partial}{\partial t_2}, \quad \frac{\partial}{\partial x} = \epsilon\frac{\partial}{\partial x_1}, \quad \phi_i = \epsilon\psi^{(0)} \tag{6}$$

with

$$\sum_i f_i^{(n)} = 0, \quad \sum_i \boldsymbol{c}_i f_i^{(n)} = 0, \quad n > 0 \tag{7}$$

By matching the scales of ϵ^0, ϵ^1, ϵ^2 and ϵ^3, and introducing $D_{1i} = \partial_{t_1} + \boldsymbol{c}_i\nabla$, we have

$$\epsilon^0 : f_i^{(0)} = f_i^{eq}, \tag{8}$$

$$\epsilon^1 : \mathrm{D}_{1i} f_i^{(0)} + \frac{f_i^{(1)}}{\tau\delta_t} = \psi_i^{(0)} \tag{9}$$

$$\epsilon^2 : \partial_{t_2} f_i^{(0)} + \mathrm{D}_{1i} f_i^{(1)} + \frac{\delta_t}{2}\mathrm{D}_{1i}^2 f_i^{(0)} + \frac{f_i^{(2)}}{\tau\delta_t} = 0 \tag{10}$$

$$\epsilon^3 : \partial_{t_3} f_i^{(0)} + \partial_{t_2} f_i^{(1)} + \mathrm{D}_{1i} f_i^{(2)} + \frac{\delta_t}{2}\mathrm{D}_{1i}^2 f_i^{(1)} + \frac{\delta_t^2}{6}\mathrm{D}_{1i}^3 f_i^{(0)} + \frac{f_i^{(3)}}{\tau\delta_t} = 0 \tag{11}$$

After some tedious algebra, the t_3 order of the continuity equation can be derived as

$$\frac{\partial \rho}{\partial t_3} + \delta_t^2(\tau - 1/3)\nabla^2(p\boldsymbol{S}^{(2)}) + \frac{\delta_t^2}{6}\nabla^3\boldsymbol{\Psi}^{(3)} = 0 \tag{12}$$

where $\mathbf{S}^{(2)} = (\nabla\mathbf{u} + \nabla^T\mathbf{u} - 2/3\nabla\cdot\mathbf{u}\mathbf{I})/2$ and $\sum_i \boldsymbol{c}_i\boldsymbol{c}_i f_i^{(1)} \approx -2\delta_t\tau p\boldsymbol{S}^{(2)}$. The continuity equation with the truncation errors can be finally obtained as follows

$$\frac{\partial \rho}{\partial t} + \nabla\cdot(\rho\boldsymbol{u}) = -\delta_t^2(\tau - 1/3)\nabla^2(p\boldsymbol{S}^{(2)}) - \frac{\delta_t^2}{6}\nabla^3\boldsymbol{\Psi}^{(3)} \tag{13}$$

It shows that the common error term of order $\mathcal{O}(\delta_t^2)$ done in solving lattice Boltzmann equation may induce an associated error term on the continuity equation. The mass conservation law is not strictly satisfied by the lattice Boltzmann method, especially with non-uniform forcing terms. By adopting different expansion techniques, truncated errors of the continuity equation may have different expressions [23,31–35]. However, it does not affect the following analysis on effect of mass conservation in the hybrid lattice Boltzmann methods. The corresponding effect of the deviation of mass conservation on energy conservation within the framework of hybrid lattice Boltzmann method is studied in the following sections.

3. Evaluation of energy conservation equations in hybrid compressible LBM

In the hybrid lattice Boltzmann method, the density is obtained from LBM. According to above analysis, the mass equation derived from LBM is not strictly identical to the usual macroscopic equation used in the Euler-Navier–Stokes framework. It can be written as:

$$\frac{\partial \rho_{\mathrm{LB}}}{\partial t} + \nabla\cdot(\rho\boldsymbol{u})_{\mathrm{LB}} = \epsilon_\rho \tag{14}$$

where the subscript LB denotes macroscopic quantities computed from the LBM kernel. On the contrary, the energy conservation equation which is solved by the FVM or FDM is the same as in Navier-Stokes equations, at least at the continuous level. In this kind of hybrid equation system, different solvers are used to solve different equations with different conservation properties. Thus, the consistency between these different equations should be assessed. The different forms of energy conservation equation associated to the various possible macroscopic quantities (e.g, entropy, internal energy and total energy) should also be addressed. In the following, we will consider the conservative form of entropy, internal energy and total energy equations within the framework of hybrid compressible LBM. Without loss of generality, the viscous terms of these equations are neglected to simplify the analysis.

3.1. Entropy equation

In numerical simulation, the solution should obey the second law of thermodynamic for entropy evolution. That is why there are lots of algorithms [36–42] based on controlling the entropy in a natural way to enforce both numerical stability and physical evolution of the entropy at the same time. Thus, the conservative entropy equation is considered first. At this point, it is worth noting that we are referring here to the physical entropy derived from the thermodynamic theory, not to a mathematical pseudo-entropy function, as done in many work devoted to the derivation of stabilized numerical methods.

When using the conservative form in the hybrid method, the governing equations for density and entropy can be written as follows:

$$\frac{\partial \rho_{\mathrm{LB}}}{\partial t} + \nabla\cdot(\rho\boldsymbol{u})_{\mathrm{LB}} = \epsilon_\rho \tag{15a}$$

$$\frac{\partial (\rho s)_{\mathrm{FV}}}{\partial t} + \nabla\cdot(s(\rho\boldsymbol{u})_{\mathrm{LB}}) = 0 \tag{15b}$$

where the subscript FV is related to quantities computed using the Finite Volume/Finite Difference method. The entropy of the system can be calculated as $s = (\rho s)_{\mathrm{FV}}/\rho_{\mathrm{LB}}$. Combining Eq. (15a) and Eq. (15b), the equivalent non-conservative entropy equation of this system is

$$\frac{\partial s}{\partial t} + \boldsymbol{u}\cdot\nabla s = -s\frac{\epsilon_\rho}{\rho}. \tag{16}$$

In the above equation, the appearance of the spurious source term $-s\epsilon_\rho/\rho$ between non-conservative form and conservative form indicates that this hybrid equation system may generate spurious entropy source/sink. Thus, the entropy equation in the conservative form is not compatible with the mass and momentum equations obtained from the LBM kernel.

It is clear that to recover a non-conservative entropy equation without error source term one needs a conservative entropy equation and a strictly conserved mass equation. To this end, an appropriate way to update the entropy could be to compute it as $s = (\rho s)_{\mathrm{FV}}/\rho_{\mathrm{FV}}$, where ρ_{FV} denotes density obtained by solving the mass conservation equation by a classical conservative Finite Volume method. Following this approach, an additional mass conservation equation should be solved by FVM to get the ρ_{FV}, leading to the following consistent equation set

$$\frac{\partial \rho_{\mathrm{LB}}}{\partial t} + \nabla\cdot(\rho\boldsymbol{u})_{\mathrm{LB}} = \epsilon_\rho \tag{17a}$$

$$\frac{\partial (\rho s)_{\mathrm{FV}}}{\partial t} + \nabla\cdot(s(\rho\boldsymbol{u})_{\mathrm{LB}}) = 0 \tag{17b}$$

$$\frac{\partial \rho_{\mathrm{FV}}}{\partial t} + \nabla\cdot((\rho\boldsymbol{u})_{\mathrm{LB}}) = 0 \tag{17c}$$

Here, the density obtained from the FVM, ρ_{FV}, is only used to update the entropy s. The momentum $\rho\boldsymbol{u}$ is computed using the LBM kernel, i.e. $\rho\boldsymbol{u} = (\rho\boldsymbol{u})_{\mathrm{LB}}$ in all equations.

Due to the fact that the mass equation in the hybrid method is not strictly conserved, the classical conservative entropy equation is not fully consistent in this hybrid system, since a error term arises from the convection term.

A new form of entropy equation is needed to get a consistent hybrid equation system. The conservative entropy equation taking into account the consistency error source term is:

$$\frac{\partial (\rho s)_{\mathrm{FV}}}{\partial t} + \nabla\cdot(s(\rho\boldsymbol{u})_{\mathrm{LB}}) = \epsilon_{\rho s} \tag{18}$$

with $\epsilon_{\rho s} = s\epsilon_\rho$ for the sake of consistency. According to Eq. (15a), one has

$$\frac{\partial (\rho s)_{\mathrm{FV}}}{\partial t} + \nabla\cdot(s(\rho\boldsymbol{u})_{\mathrm{LB}}) = s\left[\frac{\partial \rho_{\mathrm{LB}}}{\partial t} + \nabla\cdot(\rho\boldsymbol{u})_{\mathrm{LB}}\right] \tag{19}$$

Simplifying the above equation, the following form of the consistent entropy equation can be written as

$$\frac{\partial (\rho s)_{\mathrm{FV}}}{\partial t} + (\rho\boldsymbol{u})_{\mathrm{LB}}\cdot\nabla s = s\frac{\partial \rho_{\mathrm{LB}}}{\partial t} \tag{20}$$

In this hybrid method, before solving Eq. (20), $\frac{\partial \rho_{\mathrm{LB}}}{\partial t}$ has already been obtained from LBM. Thus, the only problem would be how to deal with s in the right hand side of the above equation. Using the first-order Euler scheme in temporal integral, the above equation can be written as

$$\frac{(\rho s)_{\mathrm{FV}}^{(n)} - (\rho s)_{\mathrm{FV}}^{(n-1)}}{\Delta t} + (\rho \boldsymbol{u})_{\mathrm{LB}}^{(n)} \cdot \nabla s = s^* \frac{\partial \rho_{\mathrm{LB}}}{\partial t} \tag{21}$$

It can be proved that the above equation is identical to the one obtained when discretizing the non-conservative entropy equation with the first-order Euler scheme when taking $s^* = s^{(n)}$, leading to an implicit problem. The non-conservative entropy equation has been observed to be very robust and accurate [4,5,25]. In order to further validate the idea of adding a source term in the conservative entropy equation while keeping a fully explicit method, $s^* = s^{(n-1)}$ will be used in the following.

3.2. Internal energy equation

Hybridizing the conservative internal energy equation with the LBM kernel for mass and momentum conservation, the following set of equations is obtained for perfect gas :

$$\frac{\partial \rho_{\mathrm{LB}}}{\partial t} + \nabla \cdot (\rho \boldsymbol{u})_{\mathrm{LB}} = \epsilon_\rho \tag{22a}$$

$$\frac{\partial (\rho e)_{\mathrm{FV}}}{\partial t} + \nabla \cdot (e(\rho \boldsymbol{u})_{\mathrm{LB}}) + p \nabla \cdot (\boldsymbol{u})_{\mathrm{LB}} = 0 \tag{22b}$$

where the internal energy is computed as $e = (\rho e)_{\mathrm{FV}}/\rho_{\mathrm{LB}}$, and the pressure p is computed using the perfect gas equation of state, i.e. $p = \rho_{\mathrm{LB}} e(\gamma - 1) = (\rho e)_{\mathrm{FV}}(\gamma - 1)$. As shown in [43], the entropy evolution equation can be recast using the Gibbs equation as

$$\begin{aligned} &\frac{\partial \rho s}{\partial t} + \nabla \cdot (\rho \boldsymbol{u} s) \\ &= \frac{1}{T}\left[(sT - e - \frac{p}{\rho})(\frac{\partial \rho}{\partial t} + \nabla \cdot (\rho \boldsymbol{u})) + \frac{\partial \rho e}{\partial t} + \nabla \cdot (\rho \boldsymbol{u} e) + p \nabla \cdot \boldsymbol{u} \right] \end{aligned} \tag{23}$$

Therefore, the equivalent entropy equation associated with the above system based on the internal energy is

$$\frac{\partial (\rho s)_{\mathrm{FV}}}{\partial t} + \nabla \cdot (s(\rho \boldsymbol{u})_{\mathrm{LB}}) = \epsilon_{\rho s} = s\epsilon_\rho - \frac{1}{T}(e + \frac{p}{\rho})\epsilon_\rho \neq s\epsilon_\rho \tag{24}$$

As mentioned above, the source term $\epsilon_{\rho s}$ should be equal to $s\epsilon_\rho$. Otherwise, spurious entropy source/sink terms may arise in this system. Thus, the conservative internal energy equation is not consistent with LBM.

In order to meet the condition $\epsilon_{\rho s} = s\epsilon_\rho$, a correction source term should be added to conservative internal energy equation, yielding

$$\frac{\partial (\rho e)_{\mathrm{FV}}}{\partial t} + \nabla \cdot (e(\rho \boldsymbol{u})_{\mathrm{LB}}) + p \nabla \cdot (\boldsymbol{u})_{\mathrm{LB}} = \epsilon_{\rho e} = (e + \frac{p}{\rho})\epsilon_\rho \tag{25}$$

To simplify the above equation, the divergence term $\nabla \cdot \boldsymbol{u}$ can be reconstructed as $\nabla \cdot \boldsymbol{u} = [\nabla \cdot (\rho \boldsymbol{u}) - \boldsymbol{u} \cdot \nabla \rho]/\rho$. Combining the Eq. (15a) and Eq. (25), a new form of internal energy equation which is consistent with the LBM can be derived as

$$\frac{\partial (\rho e)_{\mathrm{FV}}}{\partial t} + \rho_{\mathrm{LB}}^{\gamma-1} (\rho \boldsymbol{u})_{\mathrm{LB}} \cdot \nabla (e/\rho_{\mathrm{LB}}^{\gamma-1}) = \gamma e \frac{\partial \rho_{\mathrm{LB}}}{\partial t} \tag{26}$$

For solving the above equation, the internal energy e appearing in the right-hand-side will be treated explicitly $e = e^{n-1}$ in the following.

Eq. (26) can also be written in a non-conservative form as:

$$\frac{\partial e}{\partial t} + \rho^{\gamma-1} \boldsymbol{u} \cdot \nabla (e/\rho^{\gamma-1}) = (\gamma - 1)\frac{e}{\rho}\frac{\partial \rho_{\mathrm{LB}}}{\partial t} \tag{27}$$

By adding an additional mass conservation equation to the above equation, a consistent set of equations which is similar to Eq. (17) can be obtained:

$$\frac{\partial \rho_{\mathrm{LB}}}{\partial t} + \nabla \cdot (\rho \boldsymbol{u})_{\mathrm{LB}} = \epsilon_\rho \tag{28a}$$

$$\frac{\partial (\rho e)_{\mathrm{FV}}}{\partial t} + \rho_{\mathrm{LB}}^{\gamma-1} \nabla \cdot ((\rho \boldsymbol{u})_{\mathrm{LB}} e/\rho^{\gamma-1}) = (\gamma - 1) e \frac{\partial \rho_{\mathrm{LB}}}{\partial t} \tag{28b}$$

$$\frac{\partial \rho_{\mathrm{FV}}}{\partial t} + \nabla \cdot ((\rho \boldsymbol{u})_{\mathrm{LB}}) = 0 \tag{28c}$$

In the above system, the density obtained from the FVM is only used to update the internal energy $e = (\rho e)_{\mathrm{FV}}/\rho_{\mathrm{FV}}$. The momentum $\rho \boldsymbol{u}$ is computed by using the LBM kernel in all terms, i.e. $\rho \boldsymbol{u} = (\rho \boldsymbol{u})_{\mathrm{LB}}$.

3.3. Total energy equation

In the hybrid method, the goal of solving the energy conservation equation is to compute the temperature. If the energy equation is written in terms of entropy or internal energy, the temperature can be calculated by using density and entropy or by density and internal energy. However, the situation is different when solving the total energy equation. In this case, the temperature should be updated as $T = [(\rho E)_{\mathrm{FV}} - \frac{1}{2}(\rho k)_{\mathrm{LB}}]/(c_v \rho_{\mathrm{LB}})$, where $k = \|\boldsymbol{u}\|^2/2$. It can be observed that the temperature is directly related to the density, velocity and total energy at the same time step. Thus, this case is much more complicated than one using and discretizing entropy or internal energy equation. The kinetic energy equation which has been determined by the LBM is also involved in the total energy equation. As mentioned above, the mass equation recovered by the LBM is not strictly conserved. In a similar way, it can be very straightforwardly seen that the momentum equation obtained from the LBM is also not strictly conserved. Thus, the hybrid equation system including a conservative total energy equation can be written as follows

$$\frac{\partial \rho_{\mathrm{LB}}}{\partial t} + \nabla \cdot (\rho \boldsymbol{u})_{\mathrm{LB}} = \epsilon_\rho \tag{29a}$$

$$\frac{\partial (\rho \boldsymbol{u})_{\mathrm{LB}}}{\partial t} + \nabla \cdot (\rho \boldsymbol{u}\boldsymbol{u})_{\mathrm{LB}} + (\nabla p)_{\mathrm{LB}} = \boldsymbol{\epsilon}_{\rho u} \tag{29b}$$

$$\frac{\partial (\rho E)_{\mathrm{FV}}}{\partial t} + \nabla \cdot ((\rho \boldsymbol{u})_{\mathrm{LB}} H) = 0 \tag{29c}$$

where $E = e + k$ and $H = E + p/\rho$. As in the previous cases, the momentum is computed using the LBM kernel, i.e. $\rho \boldsymbol{u} = (\rho \boldsymbol{u})_{\mathrm{LB}}$ and $(\rho \boldsymbol{u}\boldsymbol{u})_{\mathrm{LB}} = (\rho \boldsymbol{u})_{\mathrm{LB}}(\rho \boldsymbol{u})_{\mathrm{LB}}/\rho_{\mathrm{LB}}$.

As the mass and momentum equations are not strictly conserved, the associated evolution equation for kinetic energy with an error source term is

$$\frac{\partial \rho k}{\partial t} + \nabla \cdot (\rho \boldsymbol{u} k) + \boldsymbol{u} \cdot \nabla p = \epsilon_{\rho k} = \boldsymbol{u} \cdot \boldsymbol{\epsilon}_{\rho u} - k\epsilon_\rho \tag{30}$$

Following Eq. (23), the equivalent entropy equation of this system can be recast as

$$\begin{aligned} \frac{\partial \rho s}{\partial t} + \nabla \cdot (\rho \boldsymbol{u} s) = \frac{1}{T}\Big[&(sT - H + k)(\frac{\partial \rho}{\partial t} + \nabla \cdot (\rho \boldsymbol{u})) \\ &+ \frac{\partial \rho E}{\partial t} + \nabla \cdot (\rho \boldsymbol{u} H) - \frac{\partial \rho k}{\partial t} \\ &- \nabla \cdot (\rho \boldsymbol{u} k) - \boldsymbol{u} \cdot \nabla p \Big] \end{aligned} \tag{31}$$

The source term of this entropy equation is

$$\epsilon_{\rho s} = s\epsilon_\rho - \frac{1}{T}\Big[(H - k)\epsilon_\rho + \epsilon_{\rho k} \Big] \neq s\epsilon_\rho \tag{32}$$

Therefore, the conservative total energy equation is also not consistent with the LBM kernel for mass and momentum conservation. In order to remove the additional source term in the equivalent entropy equation, the consistent total energy equation should be rewritten in the following form

$$\frac{\partial(\rho E)_{\mathrm{FV}}}{\partial t}+\nabla\cdot((\rho\boldsymbol{u})_{\mathrm{LB}}H)=\epsilon_{\rho E}=H\epsilon_{\rho}+\epsilon_{\rho k}-k\epsilon_{\rho} \tag{33}$$

It can be found that the source term of total energy equation $\epsilon_{\rho E}$ is not only related to the error term of mass equation ϵ_{ρ} but also to the error terms arising in the kinetic energy equation $\epsilon_{\rho k}$. As a consequence, it's very difficult to establish a consistent system for total energy. This issue can be simplified by neglecting the error terms $\epsilon_{\rho k}$: doing that, the source term $\epsilon_{\rho E}$ can be evaluated with the help of additional mass conservation equation, leading to

$$\begin{aligned}&\frac{\partial\rho_{\mathrm{FV}}}{\partial t}+\nabla\cdot((\rho\boldsymbol{u})_{\mathrm{LB}})=0\\&\frac{\partial(\rho E)_{\mathrm{FV}}}{\partial t}+\nabla\cdot((\rho\boldsymbol{u})_{\mathrm{LB}}H)=\gamma e(\rho_{\mathrm{LB}}-\rho_{\mathrm{FV}})\end{aligned} \tag{34}$$

Comparing this simplified total energy equation with the Eq. (29), it is seen that the error term of mass equation is taken into account in the above equation. Therefore, it is better than the original conservative total energy equation, since it is partially corrected.

Since Eq. (34) is not fully consistent with the LBM, the error term $\epsilon_{\rho k}$ needs to be expressed to recover a fully consistent total energy equation. Following the above idea of solving additional equation, the additional mass and momentum conservation equations solved by the FVM are both required here to recover the error terms ϵ_{ρ} and $\epsilon_{\rho\mathbf{u}}$. However, there is no interest for using the hybrid method since the density, velocity and temperature can be all obtained from the FVM. For the sole sake of theoretical investigation of the consistency errors, when using the mass and momentum equations given in Eq. (29) to recover the error terms, one can get the following equation by substituting ϵ_{ρ} and $\boldsymbol{\epsilon}_{\rho u}$ into Eq. (33):

$$\begin{aligned}&\frac{\partial(\rho E)_{\mathrm{FV}}}{\partial t}+\rho_{\mathrm{LB}}^{\gamma-1}(\rho\boldsymbol{u})_{\mathrm{LB}}\cdot\nabla(e/\rho^{\gamma-1})\\&\quad=\gamma e\frac{\partial\rho_{\mathrm{LB}}}{\partial t}+\boldsymbol{u}\cdot\frac{\partial(\rho\boldsymbol{u})_{\mathrm{LB}}}{\partial t}-k\frac{\partial\rho_{\mathrm{LB}}}{\partial t}\end{aligned} \tag{35}$$

As $\frac{\partial\rho k}{\partial t}=\mathbf{u}\frac{\partial\rho\mathbf{u}}{\partial t}-k\frac{\partial\rho}{\partial t}$, It can be proved that the above equation is identically equal to the consistent internal energy Eq. (26).

4. Numerical experiments: results and discussion

In the above section, the consistency between the energy conservation equations and the LBM has been addressed. It can be found theoretically that the conservative forms of entropy, internal energy and total energy equation could induce spurious entropy sink/source terms. In order to reduce these erroneous entropy terms, some correction terms have been proposed to recover consistent energy equations based on entropy and internal energy.

In the following, these theoretical analyses and corrected equations will be assessed in several numerical simulations by using the hybrid recursive regularized lattice Boltzmann method (HRR-LBM). In the HRR-LBM, the second-order off-equilibrium moment can be calculated as $\mathcal{A}_{\alpha\beta}^{(1,\mathrm{HRR})}=\sigma\mathcal{A}_{\alpha\beta}^{(1)}+(1-\sigma)\mathcal{A}_{\alpha\beta}^{(1,\mathrm{FD})}$. $\sigma\in[0,1]$ is an arbitrary weighting coefficient. $\mathcal{A}_{\alpha\beta}^{(1,\mathrm{FD})}$ is estimated by its Chapman-Enskog solution which is approximated by a second-order finite-difference scheme. The details of the HRR-LBM can be found in [5,25,44]. In the simulations, the inviscid flows are treated as flows with vanishing viscosity, i.e. taking $\mu=10^{-15}$.

The results obtained using the consistent equation sets Eq. (17) and Eq. (28) will be denoted by $(\rho s)_c$ and $(\rho e)_c$, respectively. The notations $(\rho s)_*$ and $(\rho e)_*$ are related to results obtained using the corrected consistent energy equations given in Eq. (20) and Eq. (26). The original conservative, uncorrected and inconsistent forms of entropy, internal energy and total energy equations will be displayed as $(\rho s)_o$, $(\rho e)_o$ and $(\rho E)_o$. The results obtained using the partially corrected Eq. (34) will be plotted as $(\rho E)_{nc}$. The summary of these equations is presented in Table 2.

4.1. Isentropic vortex convection

The problem of inviscid isentropic vortex convection is investigated using the different energy conservation equations discussed above. The size of the computational domain is $[0,10]\times[0,10]$. The free-stream parameters are $\rho_\infty=1$, $v_\infty=0$, $p_\infty=1$, $u_\infty=Ma_\infty\sqrt{\gamma p_\infty/\rho_\infty}$. Here, two cases are considered with $Ma_\infty=0$ (stationary vortex) and $Ma_\infty=0.845$ (vortex advected by a uniform base flow), respectively. Initially, the following disturbance is added to the above free-stream:

$$\rho=\left[1-\frac{(\gamma-1)b^2}{8\gamma\pi^2}e^{1-r^2}\right]^{\frac{1}{\gamma-1}},\quad p=\rho^{\gamma}, \tag{36}$$

$$u=u_\infty-\frac{b}{2\pi}e^{\frac{1}{2}(1-r^2)}(y-y_c), \tag{37}$$

$$v=v_\infty+\frac{b}{2\pi}e^{\frac{1}{2}(1-r^2)}(x-x_c). \tag{38}$$

where $b=0.5, x_c=5, y_c=5$ and $r=\left[(x-x_c)^2+(y-y_c)^2\right]^{1/2}$. The HRR weighting parameter is set to $\sigma=0.5$. In all simulations, the grid size is $\delta x=0.05$ and time step is $\delta t=0.01$. In all directions, periodic boundary conditions are implemented. Thus, this test case is a very appropriate one to check if the energy conservation equation which is hybridized with LBM can induce spurious entropy sources/sinks.

Fig. 1 shows the density fields obtained using the different energy equations at $Ma_\infty=0$. It can be observed that the conservative forms of total energy and internal energy are quite unstable (e.g., total energy is displayed). The result in Fig. 1(b) is totally polluted at time $t=5$. For the conservative entropy equation, we can get the stable result at time $t=500$ (Fig. 1(f)). However, this result is not correct compared with the analytical solution. By using the consistent and corrected energy equations, stable and satisfactory results are obtained in Fig. 1(d)(e)(g)(h) at $t=500$. For the partially corrected total energy Eq. (34), as mentioned above, the error terms of kinetic energy equation $\epsilon_{\rho k}$ is not balanced. From Eq. (30), it can be found that the value of $\epsilon_{\rho k}$ is related to $\mathbf{u}$. In this test case, since $Ma_\infty=0$, $\epsilon_{\rho k}$ is very small. Thus, we still get the stable and reliable results at $t=500$ for $Ma_\infty=0$.

For the sake of a quantitative measure of the quality of the solutions, the time evolution of L_2 errors are plotted in Fig. 2. The L_2 error is defined as

$$L_2=\sqrt{\frac{\int_A(\phi-\phi_{exact})^2\mathrm{dxdy}}{A}} \tag{39}$$

where A is the area of the computational domain. It is observed that the L_2 errors of non-corrected conservative forms of total energy and internal energy are out of control after a very short time. For the conservative entropy equation, the L_2 errors are stable and bounded, but the observed values are quite large. For the corrected and consistent energy equations, following the theoretical analysis, the L_2 errors are very small. The L_2 errors of the partially corrected total energy equation are much smaller than those by original conservative total energy equation. However, as $\epsilon_{\rho k}$ is not equal

Table 2
Summarizing of formulation of energy equation.

			notation	mass	momentum	energy
formulation of energy equation	entropy	original	$(\rho s)_o$	LB	LB	FV (15b)
		consistent	$(\rho s)_c$	LB	LB	FV (17)
		corrected	$(\rho s)_*$	LB	LB	FV (20)
	internal energy	original	$(\rho e)_o$	LB	LB	FV (22b)
		consistent	$(\rho e)_c$	LB	LB	FV (28)
		corrected	$(\rho e)_*$	LB	LB	FV (26)
	total energy	original	$(\rho E)_o$	LB	LB	FV (29c)
		corrected	$(\rho E)_{nc}$	LB	LB	FV (34)

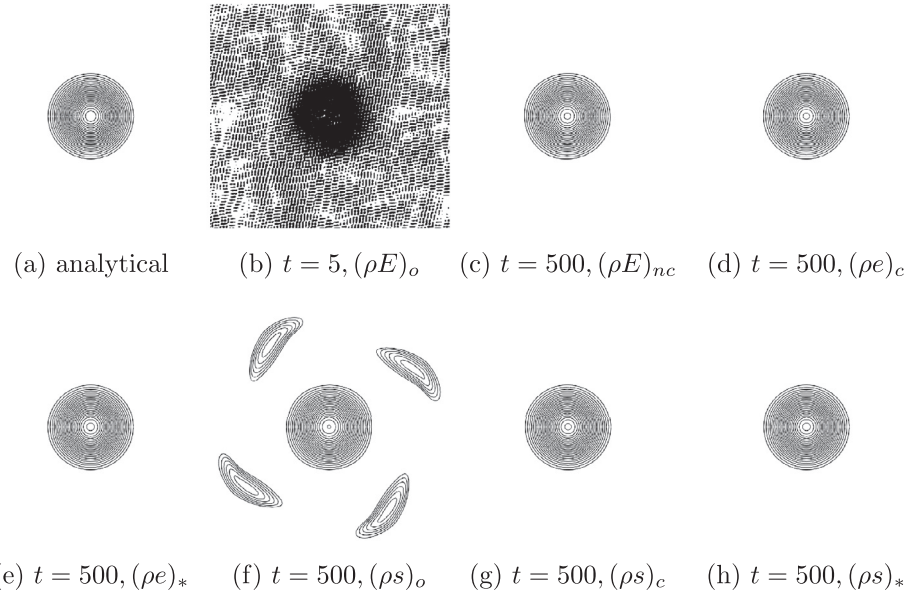

(a) analytical (b) $t = 5, (\rho E)_o$ (c) $t = 500, (\rho E)_{nc}$ (d) $t = 500, (\rho e)_c$

(e) $t = 500, (\rho e)_*$ (f) $t = 500, (\rho s)_o$ (g) $t = 500, (\rho s)_c$ (h) $t = 500, (\rho s)_*$

Fig. 1. Density fields. The contours are from 0.993 to 0.999 with 30 levels.

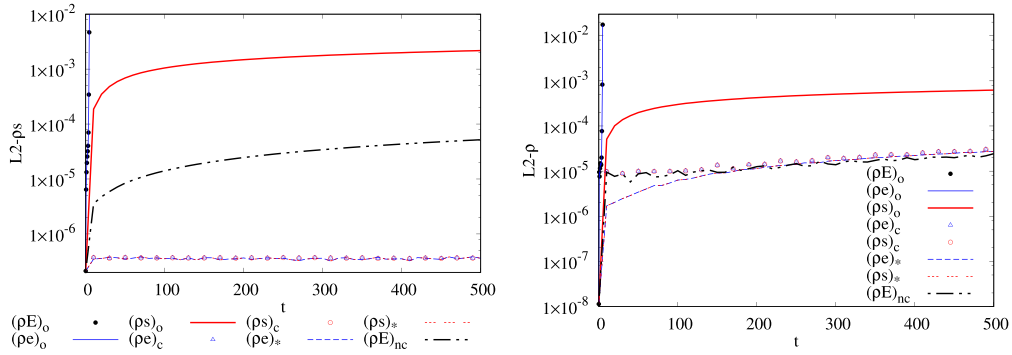

(a) L_2 error of total entropy (b) L_2 error of density

Fig. 2. The L_2 error of $Ma_\infty = 0$.

to zero, the entropy L_2 error in this case is larger than those of the corrected and consistent energy equations. For further comparisons, the distributions of density and velocity on the mid-line at time $t = 500$ are shown in Fig. 3. It can be found that the density distribution of conservative entropy equation is totally wrong compared with the exact solution.

For the case with $Ma_\infty = 0.845$, the L_2 errors are displayed in Fig. 4. It can be observed that L_2 errors obtained by the conservative form of entropy and internal energy equation grow very fast. However, the errors of the corrected and consistent equations are quite small even after $50T$. It should be noticed that the results of partially corrected total energy equation are not stable anymore as the error term $\epsilon_{\rho k}$ is not negligible at $Ma_\infty = 0.845$. At $t = 50T$, the distributions of density and velocity obtained by the corrected equations are plotted in Fig. 5. It is found that these results are quite close to the exact solutions. These results are in a very good agreement with the theoretical analysis.

4.2. Taylor-Green vortex

The inviscid compressible Taylor-Green vortex is widely used to test the robustness and accuracy of the various discretizations of convective terms in Navier–Stokes equations [39,40,45]. In this

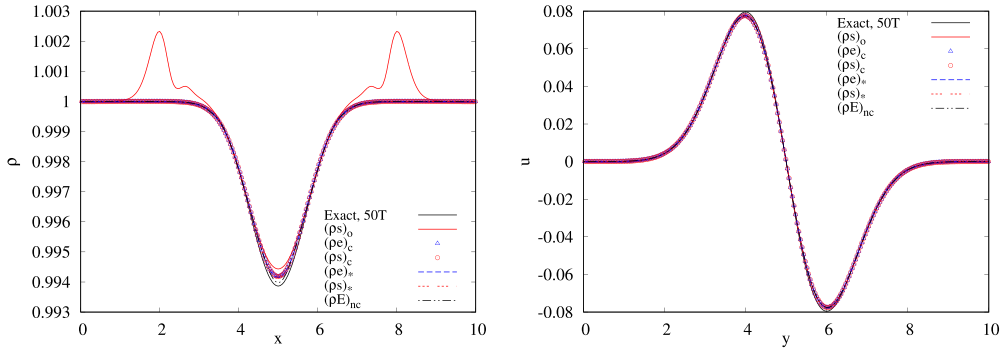

(a) Density (b) Velocity

Fig. 3. The distributions of density and velocity on the mid-line at $t = 500$ ($Ma_\infty = 0$).

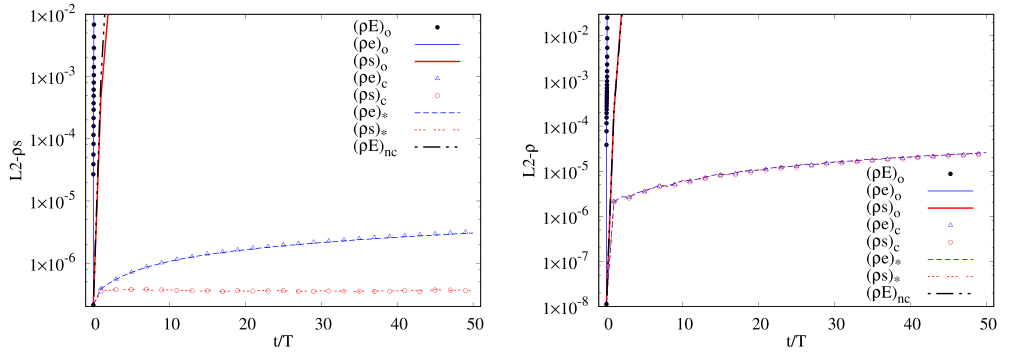

(a) L_2 error of total entropy (b) L_2 error of density

Fig. 4. The L_2 error of $Ma_\infty = 0.845$.

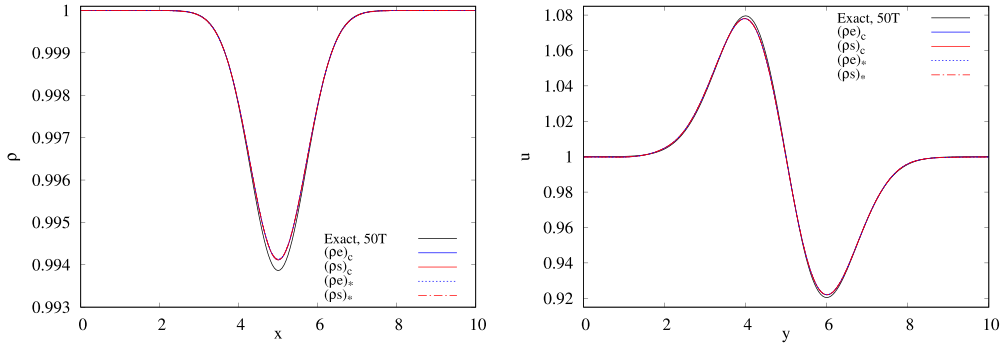

(a) Density (b) Velocity

Fig. 5. The distributions of density and velocity on the mid-line at $t = 50T$ ($Ma_\infty = 0.845$).

test case, the computational domain is $x \in [0, 2\pi] \times y \in [0, 2\pi] \times z \in [0, 2\pi]$. On the x, y and z directions of the computational domain, the periodic boundary conditions are implemented. The initial conditions are as follows:

$$\begin{aligned} p_0 &= p_b + [(\cos 2x + \cos 2y)(\cos 2z + 2) - 2]/16 \\ \rho_0 &= \rho_b,\ T_0 = p_0/\rho_0,\ U_b = Ma_b\sqrt{\gamma\, p_b/\rho_b} \\ u_0 &= U_b \sin x \cos y \cos z,\ v_0 = -U_b \cos x \sin y \cos z \\ w_0 &= 0,\ p_b = 100,\ \rho_b = 1,\ Ma_b = 0.0845 \end{aligned} \tag{40}$$

We use 32^3 grids to discretize the computational domain. The time step δt is equal to 0.01. The final time is $t = 50$. The parameter σ in the HRR collision model is taken equal to 0.95.

The conservation properties of the formulations discussed above are investigated by checking the conservation of physical global invariant quantities. In the limit of vanishing viscosity and diffusivity and in the absence of volumic source terms, the continuous equations are known to admit both linear and non linear global invariants in fully periodic domains [36,38,39,46].

Therefore, defining the integrated value $\langle\phi\rangle$ as

$$\langle\phi\rangle = \int_V \phi \ \mathrm{dxdydz}, \tag{41}$$

one can see that both $\langle\rho\phi\rangle$ and $\langle\rho\phi^2\rangle$ are time-independent invariant quantities, referred to as linear and quadratic invariants, respectively. The instantaneous spatial fluctuations around the in-

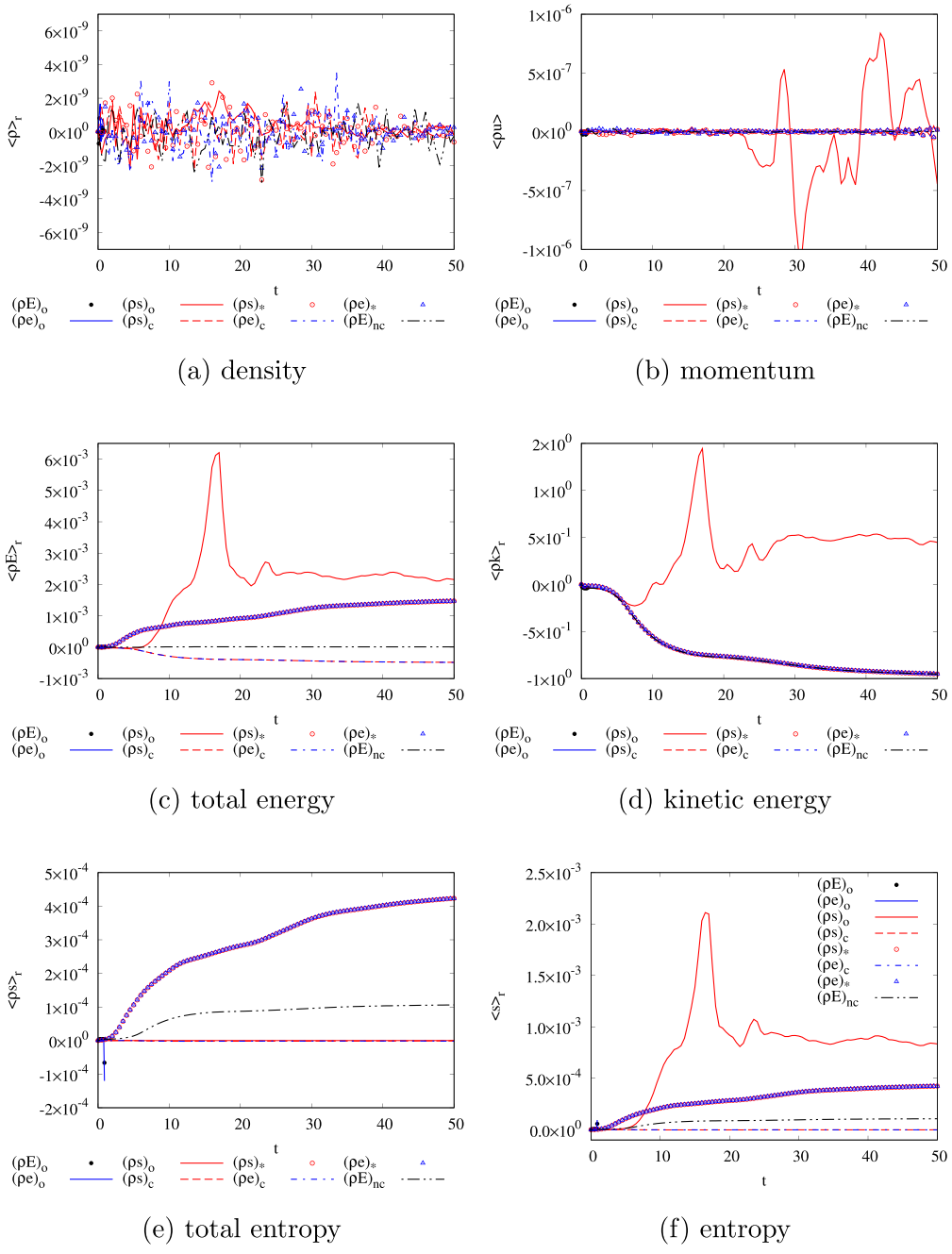

Fig. 6. Time evolution of linear global inviscid invariants.

stantaneous spatially averaged mean value are measured considering the r.m.s. estimator:

$$\langle\phi\rangle_r = (\langle\phi\rangle - \langle\phi_0\rangle)/\langle\phi_0\rangle \tag{42}$$

The results of the linear and quadratic invariants obtained by different hybrid equation systems are plotted in Fig. 6 and Fig. 7, respectively. The summary of these results is shown in Table 3.

For the terms of numerical stability or instability, at least within the time integration interval. It can be found that among the various forms of energy equations, only the original conservative equations $(\rho e)_o$ and $(\rho E)_o$ are unstable (Fig. 6(e)(f), Fig. 7(a)(b)).

For the conservative entropy equation, the total entropy ρs is conserved globally (see in Fig. 6(e)). However, as mentioned above, an uncontrollable source term exists in the equivalent entropy equation (Eq. (16)) for the conservative entropy equation. Thus, in Fig. 6(f), $\langle s\rangle_r$ of conservative entropy is very large and unreasonable. This situation can also be found in the results of $\langle\rho s^2\rangle_r$ and $\langle\rho E^2\rangle_r$ in Fig. 7. These erroneous entropy productions/reductions also induce erroneous results of $\langle\rho E\rangle_r$, $\langle\rho k\rangle_r$ and $\langle\rho u\rangle$. For the non-fully consistent total energy equation, as Mach number of this problem is small ($Ma_b = 0.0845$), it is consistent with the LBM. The results of $(\rho E)_{nc}$ are stable and associated values kept in the small values.

For the consistent and corrected energy equations, all the results are stable. It is worth to mention that the results of $(\rho s)_c$ and $(\rho e)_c$ are better than those of $(\rho s)_*$ and $(\rho e)_*$. The reason is that the convection part in $(\rho s)_c$ and $(\rho e)_c$ are written in the conservative forms. Fig. 8 and 9 are the results of Q-criterion obtained using the different energy equations at time $t = 4$ and 8, respectively. It can be observed that the result of conservative en-

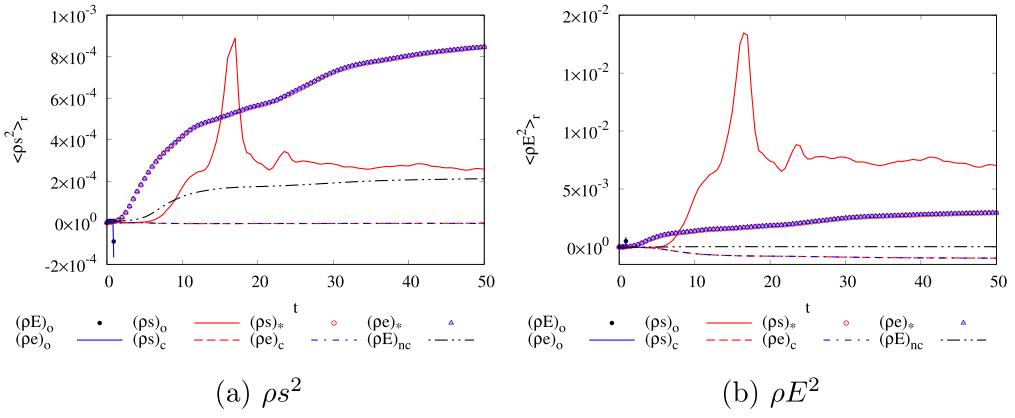

(a) ρs^2 (b) ρE^2

Fig. 7. Time evolution of quadratic global inviscid invariants.

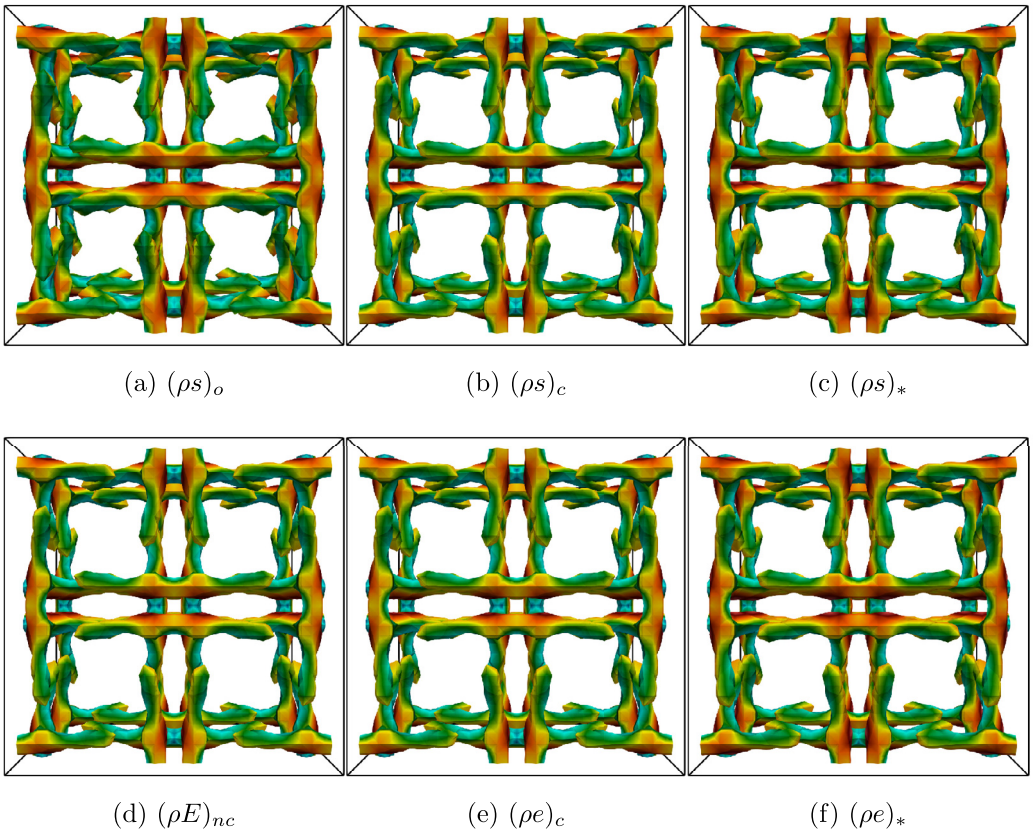

(a) $(\rho s)_o$ (b) $(\rho s)_c$ (c) $(\rho s)_*$

(d) $(\rho E)_{nc}$ (e) $(\rho e)_c$ (f) $(\rho e)_*$

Fig. 8. The isosurface of Q-criterion=1 coloured with the kinetic energy at time $t = 4$.

Table 3
Summarizing of the results obtained using different formulations of energy equation for inviscid Taylor-Green flow numerical simulations. ⊙ numerically stable, conserved globally, conserved with less than 0.1% error; ◯ numerically stable, bounded, with variations more than 0.1%; X numerically unstable. Refer to Table 2 for the definition of the various forms of the energy equations.

		Conserved variable							
		ρ	ρu	ρs	ρE	s	ρk	ρs^2	ρE^2
Formulation of energy equation	$(\rho s)_o$	⊙	⊙	⊙	◯	◯	◯	⊙	◯
	$(\rho e)_o$	X	X	X	X	X	X	X	X
	$(\rho E)_o$	X	X	X	X	X	X	X	X
	$(\rho s)_c$	⊙	⊙	⊙	⊙	⊙	◯	⊙	⊙
	$(\rho e)_c$	⊙	⊙	⊙	⊙	⊙	◯	⊙	⊙
	$(\rho s)_*$	⊙	⊙	⊙	◯	⊙	◯	⊙	◯
	$(\rho e)_*$	⊙	⊙	⊙	◯	⊙	◯	⊙	◯
	$(\rho E)_{nc}$	⊙	⊙	⊙	⊙	⊙	◯	⊙	⊙

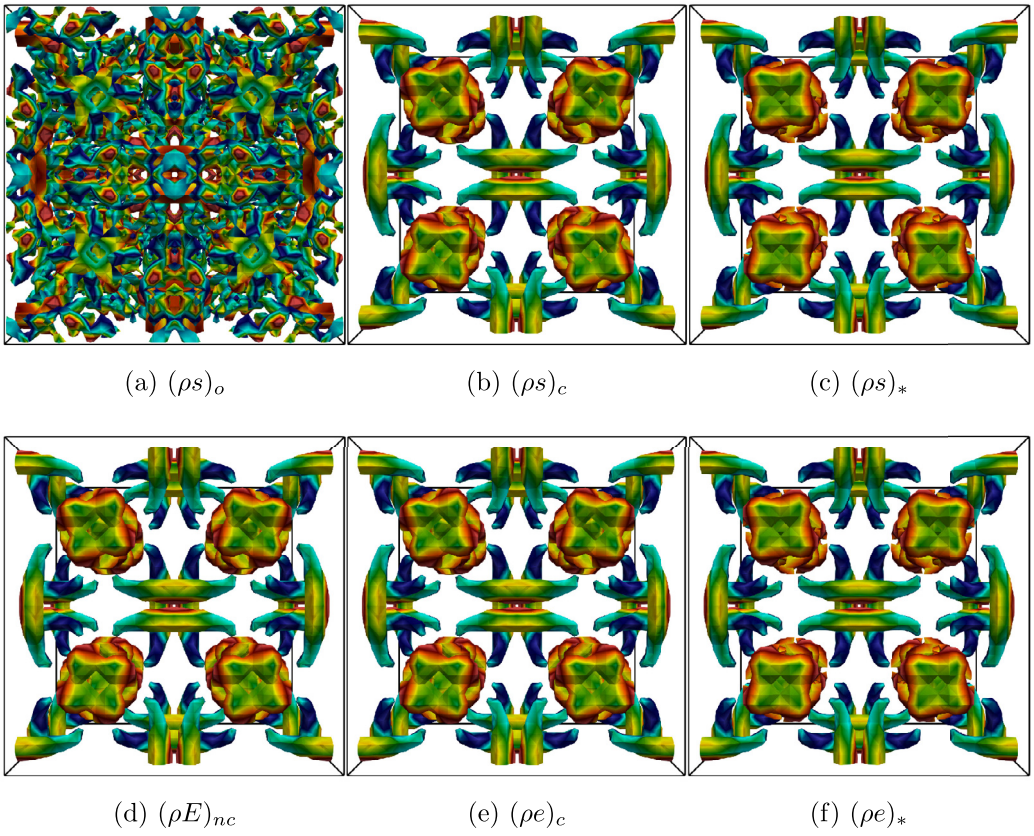

Fig. 9. The isosurface of Q-criterion=1 coloured with the kinetic energy at time $t = 8$.

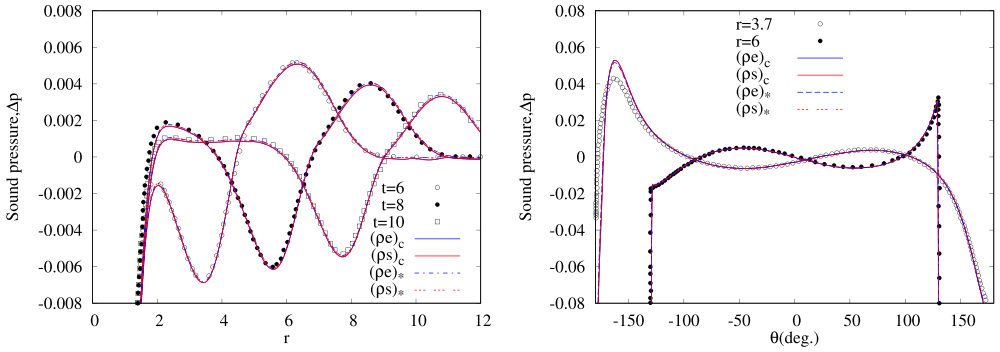

(a) Radial distribution (b) Circumferential distribution

Fig. 10. Radial and circumferential distributions of the sound pressure.

tropy equation is normal and similar with other results at $t = 4$. However, due to the erroneous entropy source term, this result is polluted and unreasonable at $t = 8$.

4.3. Shock-vortex interaction

As validated above, the inconsistency between mass, momentum equations by the LBM and energy equations by the FVM could induce erroneous entropy productions/reductions. Thus, we proposed the consistent and corrected energy equations $(\rho s)_c$, $(\rho e)_c$, $(\rho s)_*$ and $(\rho e)_*$. Here, the shock-vortex interaction problem is used to test the robustness and accuracy of these consistent energy equations on simulating both shock wave and vortex. In this test case, the upstream Mach number of the stationary normal shock wave is $M_s = 1.2$. The Mach number of the vortex is $M_v = 0.25$. The initial density, pressure, tangential and radial velocities of the vortex are given as

$$\rho_\theta(r) = [1 - \frac{\gamma - 1}{2} M_v^2 r \exp(1 - r^2)]^{\frac{1}{\gamma - 1}} \quad p(r) = \frac{1}{\gamma}\rho^\gamma(r). \tag{43}$$

$$u_\theta(r) = M_v r \exp[(1 - r^2)/2] \quad u_r(r) = 0. \tag{44}$$

where the distance from the vortex core r is non-dimensionalized by the vortex radius $R = 1$, $\gamma = 1.4$. The Reynolds number is $Re = 800$ which is defined as $Re = \rho_R a_R/\mu$. Here, the subscript R denotes the upstream of the shock wave.

The computational domain is [-20, 8]×[-12, 12]. Initially, the location of the vortex is $(x, y)_v = (2, 0)$. The stationary normal shock is specified at $x = 0$. 1120×960 grids are used in this simulation with the time step $\delta_t = 0.00833$.

Fig. 10 shows the radial and circumferential distributions of the sound pressure Δp. Here, the sound pressure is defined as $\Delta p = (p - p_L)/p_L$. The subscript L denotes the downstream of the shock wave. From the figure, it can be observed that all the results of the consistent energy equations are matched very well with the reference results [47]. These results indicate that the consistent energy equations derived from above are robust and accurate.

5. Conclusions

Based on the hybrid compressible lattice Boltzmann method, the consistency between energy conservation equations based on various thermodynamics variables and lattice Boltzmann equation has been investigated. It is found from the theoretical analysis that the conservative forms of entropy, internal energy and total energy equations in the hybrid LBM-FVM for compressible flows could induce erroneous entropy productions/reductions. By applying the theoretical analysis, a set of corrected consistent energy equations in entropy and internal energy form is proposed to reduce the error terms and improve the consistency. The theoretical analysis and revised energy equations are evaluated by the numerical test cases. The numerical results show that the corrected and consistent energy equations proposed in this paper have very good property in terms of robustness and accuracy in the framework of the hybrid lattice Boltzmann method. From a more fundamental point of view, it is shown that the choice of the thermodynamic variable has a strong influence of the conservation of linear and nonlinear invariants in the inviscid limit. The results obtained on the compressible Taylor-Green vortex show that hybrid LBM has very good preservation properties when correction terms are used to recover consistency between the LBM kernel and the energy equation.

Declaration of Competing Interest

This manuscript has not been submitted to, nor is under review at, another journal or other publishing venue.

The authors have no affiliation with any organization with a direct or indirect financial interest in the subject matter discussed in the manuscript.

CRediT authorship contribution statement

S. Guo: Methodology, Validation, Visualization, Writing - original draft. **Y. Feng:** Conceptualization, Investigation, Methodology, Writing - original draft. **P. Sagaut:** Supervision, Conceptualization, Writing - original draft.

Acknowledgements

This work was granted access to the HPC resources of Aix-Marseille Université financed by the project Equip@Meso (ANR-10-EQPX-29-01) of the program Investissements d'Avenir supervised by the Agence Nationale de la Recherche. This work was supported by project of ProLB software (http://www.prolb-cfd.com). Part of this research was supported by ANR, Renault, Airbus and SafranTech by the Industrial Chair Program ALBUMS (ANR-CHIND-18-ALBUMS).

References

[1] Lallemand P, Luo LS. Hybrid finite-difference thermal lattice Boltzmann equation. International Journal of Modern Physics B 2003;17:41–7.
[2] Tölke J. A thermal model based on the lattice Boltzmann method for low Mach number compressible flows. J Comput Theor Nanosci 2006;3(4):579–87.
[3] Gupta A, Sbragaglia M, Scagliarini A. Hybrid lattice Boltzmann/finite difference simulations of viscoelastic multicomponent flows in confined geometries. J Comput Phys 2015;291:177–97.
[4] Nie X, Shan X, Chen H. A lattice-Boltzmann/finite-difference hybrid simulation of transonic flow, in. In: 47th AIAA Aerospace Sciences Meeting Including the New Horizons Forum and Aerospace Exposition; 2009. p. 139.
[5] Feng Y, Boivin P, Jacob J, Sagaut P. Hybrid recursive regularized thermal lattice Boltzmann model for high subsonic compressible flows. J Comput Phys 2019;394:82–99.
[6] Mezrhab A, Bouzidi M, Lallemand P. Hybrid lattice-Boltzmann finite-difference simulation of convective flows. Computers & Fluids 2004;33(4):623–41.
[7] Sun Y, Zhang X. A hybrid strategy of lattice Boltzmann method and finite volume method for combined conduction and radiation in irregular geometry. Int J Heat Mass Transf 2018;121:1039–54.
[8] Marenduzzo D, Orlandini E, Cates M, Yeomans J. Steady-state hydrodynamic instabilities of active liquid crystals: hybrid lattice Boltzmann simulations. Physical Review E 2007;76(3):031921.
[9] Li Q, Kang Q, Francois MM, He Y, Luo K. Lattice Boltzmann modeling of boiling heat transfer: the boiling curve and the effects of wettability. Int J Heat Mass Transf 2015;85:787–96.
[10] Nee A. Hybrid lattice Boltzmann-finite difference formulation for combined heat transfer problems by 3D natural convection and surface thermal radiation. Int J Mech Sci 2020:105447.
[11] Bettaibi S, Kuznik F, Sediki E. Hybrid LBM-MRT model coupled with finite difference method for double-diffusive mixed convection in rectangular enclosure with insulated moving lid. Physica A 2016;444:311–26.
[12] Qin F, Carro LD, Moqaddam AM, Kang Q, Brunschwiler T, Derome D, et al. Study of non-isothermal liquid evaporation in synthetic micro-pore structures with hybrid lattice Boltzmann model. J Fluid Mech 2019;866:33–60.
[13] Wang L, Yang X, Huang C, Chai Z, Shi B. Hybrid lattice Boltzmann-TVD simulation of natural convection of nanofluids in a partially heated square cavity using buongiorno's model. Appl Therm Eng 2019;146:318–27.
[14] Hosseini SA, Safari H, Darabiha N, Thévenin D, Krafczyk M. Hybrid lattice Boltzmann-finite difference model for low Mach number combustion simulation. Combust Flame 2019;209:394–404.
[15] Yu X, Regenauer-Lieb K, Tian FB. A hybrid immersed boundary-lattice Boltzmann/finite difference method for coupled dynamics of fluid flow, advection, diffusion and adsorption in fractured and porous media. Computers & geosciences 2019;128:70–8.
[16] Filippova O, Hänel D. A novel lattice BGK approach for low Mach number combustion. J Comput Phys 2000;158(2):139–60.
[17] Chakraborty S, Chatterjee D. An enthalpy-based hybrid lattice-Boltzmann method for modelling solid–liquid phase transition in the presence of convective transport. J Fluid Mech 2007;592:155–75.
[18] Guo Z, Zheng C, Shi B. Discrete lattice effects on the forcing term in the lattice Boltzmann method. Physical review E 2002;65(4):046308.
[19] Mohamad A, Kuzmin A. A critical evaluation of force term in lattice Boltzmann method, natural convection problem. Int J Heat Mass Transf 2010;53(5):990–6.
[20] Silva G. Discrete effects on the forcing term for the lattice Boltzmann modeling of steady hydrodynamics. Computers & Fluids 2020;203:104537. doi:10.1016/j.compfluid.2020.104537.
[21] Li Q, Luo KH. Effect of the forcing term in the pseudopotential lattice Boltzmann modeling of thermal flows. Physical Review E - Statistical, Nonlinear, and Soft Matter Physics 2014;89(5):1–7.
[22] Rosis AD. Central-moments-based lattice Boltzmann schemes with force-enriched equilibria. {EPL} (Europhysics Letters) 2017;117(3):34003. doi:10.1209/0295-5075/117/34003.
[23] Huang R, Wu H, Adams NA. Density gradient calculation in a class of multiphase lattice Boltzmann models. Phys Rev E 2019;100:043306. doi:10.1103/PhysRevE.100.043306.
[24] Dellar PJ. An interpretation and derivation of the lattice Boltzmann method using strang splitting. Computers and Mathematics with Applications 2013;65:129–41.
[25] Guo S, Feng Y, Jacob J, Renard F, Sagaut P. An efficient lattice Boltzmann method for compressible aerodynamics on D3Q19 lattice. J Comput Phys 2020:109570.
[26] Casalino D, Hazir A, Mann A. Turbofan broadband noise prediction using the lattice Boltzmann method. AIAA Journal 2017:609–28.
[27] Romani G, Casalino D. Rotorcraft blade-vortex interaction noise prediction using the lattice-Boltzmann method. Aerosp Sci Technol 2019;88:147–57.
[28] Chen SY, Doolen GD. Lattice Boltzmann method for fluid flows. Annu Rev Fluid Mech 1998;30:329–64.
[29] Qian Y-H, d'Humières D, Lallemand P. Lattice BGK models for Navier-Stokes equation. EPL (Europhysics Letters) 1992;17(6):479.
[30] He XY, Chen SY, Doolen GD. A novel thermal model for the lattice Boltzmann method in incompressible limit. J Comput Phys 1998;146:282–300.
[31] Qian Y-H, Zhou Y. Higher-order dynamics in lattice-based models using the Chapman-Enskog method. Physical Review E 2000;61(2):2103.
[32] Holdych DJ, Noble DR, Georgiadis JG, Buckius RO. Truncation error analysis of lattice Boltzmann methods. J Comput Phys 2004;193(2):595–619. doi:10.1016/j.jcp.2003.08.012.
[33] Huang R, Wu H. Third-order analysis of pseudopotential lattice Boltzmann model for multiphase flow. J Comput Phys 2016;327:121–39. doi:10.1016/j.jcp.2016.09.030.
[34] Wu Y, Gui N, Yang X, Tu J, Jiang S. Fourth-order analysis of force terms in multiphase pseudopotential lattice Boltzmann model. Computers & Mathematics with Applications 2018;76(7):1699–712. doi:10.1016/j.camwa.2018.07.022.
[35] Bauer M, Silva G, Rüde U. Truncation errors of the D3Q19 lattice model for the

lattice Boltzmann method. J Comput Phys 2020;405:109111. doi:10.1016/j.jcp.2019.109111.
[36] Honein AE, Moin P. Higher entropy conservation and numerical stability of compressible turbulence simulations. J Comput Phys 2004;201(2):531–45.
[37] Levasseur V, Sagaut P, Chalot F, Davroux A. An entropy-variable-based VMS/GLS method for the simulation of compressible flows on unstructured grids. Comput Methods Appl Mech Eng 2006;195(9–12):1154–79.
[38] Kuya Y, Totani K, Kawai S. Kinetic energy and entropy preserving schemes for compressible flows by split convective forms. J Comput Phys 2018;375:823–53.
[39] Coppola G, Capuano F, Pirozzoli S, de Luca L. Numerically stable formulations of convective terms for turbulent compressible flows. J Comput Phys 2019;382:86–104.
[40] Abe Y, Morinaka I, Haga T, Nonomura T, Shibita H, Miyaji K. Stable, non-dissipative, and conservative flux-reconstruction schemes in split forms. J Comput Phys 2018;353:193–227.
[41] Chan J. On discretely entropy conservative and entropy stable discontinuous Galerkin methods. J Comput Phys 2018;362:346–74.
[42] Frapolli N. Entropic lattice Boltzmann models for thermal and compressible flows. ETH Zurich; 2017. Ph.d. thesis.
[43] Subbareddy PK, Candler GV. A fully discrete, kinetic energy consistent finite-volume scheme for compressible flows. J Comput Phys 2009;228(5):1347–64.
[44] Feng Y, Guo S, Jacob J, Sagaut P. Solid wall and open boundary conditions in hybrid recursive regularized lattice Boltzmann method for compressible flows. Physics of Fluids 2019;31(12):126103.
[45] Sjögreen B, Yee H. High order entropy conservative central schemes for wide ranges of compressible gas dynamics and MHD flows. J Comput Phys 2018;364:153–85.
[46] Veldman AE. A general condition for kinetic-energy preserving discretization of flow transport equations. J Comput Phys 2019;398:108894. doi:10.1016/j.jcp.2019.108894.
[47] Inoue O, Hattori Y. Sound generation by shock–vortex interactions. J Fluid Mech 1999;380:81–116.